Journal of Computational Physics **165,** 694–716 (2000)
doi:10.1006/jcph.2000.6627, available online at http://www.idealibrary.com on IDEAL®

On the Computation of the Eigenproblems of Hydrogen and Helium in Strong Magnetic and Electric Fields with the Sparse Grid Combination Technique

Jochen Garcke and Michael Griebel

Institut für Angewandte Mathematik, Universität Bonn, Wegelerstr. 6, D-53115 Bonn, Germany
E-mail: garckej@iam.uni-bonn.de, griebel@iam.uni-bonn.de

Received March 6, 2000; revised September 5, 2000

We introduce the combination technique for the numerical solution of d-dimensional eigenproblems on sparse grids. Here, $O(d \cdot (\log N)^{d-1})$ different problems, each of size $O(N)$, have to be solved independently. This is in contrast to the one problem of size $O(N^d)$ for a conventional finite element discretization, where N denotes the number of grid points in one coordinate direction. Therefore, also higher dimensional eigenvalue problems can be treated by our sparse grid combination approach. We apply this method to solve the three-dimensional Schrödinger equation for hydrogen (one-electron problem) and the six-dimensional Schrödinger equation for helium (two-electron problem) in strong magnetic and electric fields.

Key Words: Schrödinger equation; sparse grids; combination technique; hydrogen atom; helium atom; eigenvalue solver; numerical computation; strong magnetic fields; strong electric fields.

1. INTRODUCTION

In the late 1960s evidence for the existence of strong magnetic fields in the vicinity of white dwarf stars (10^2–10^5 T) and neutron stars (10^7–10^9 T) was found. These strong to very strong magnetic fields induce drastic changes in the atomic structure of the influenced matter. Therefore atomic properties such as energy-levels and wavelengths need to be reconsidered for matter under these conditions.

For hydrogen atoms in magnetic fields, numerical calculations for a wide range of states and field strengths have been done and the corresponding eigenvalues and eigenfunctions are known precisely; see [32, 39, 41] and the references cited therein. These results were compared to observational data and thus delivered evidence for the existence of hydrogen

0021-9991/00 $35.00

in the atmospheres of white dwarves and neutron stars with corresponding magnetic field strengths. The case of hydrogen in magnetic fields is considered solved.

The situation is different for helium atoms in strong magnetic fields. First calculations for some atomic properties with the needed precision have been performed only recently; see [7] or [8] and the references cited therein. There, either a two-particle basis composed of one-particle states of a special Gaussian basis set is used [7] or a combination of the hyperspherical close coupling approach and a finite element method of quintic order [8] is employed. In any case the six dimensions of the original Schrödinger equation for two electrons are brought down to three dimensions using symmetry arguments. However, these techniques can no longer be applied in cases where both a magnetic and an electric field are present.

In this paper, we propose to directly deal with the six-dimensional eigenvalue problem resulting from the Born–Oppenheimer approximation of the helium atom. Here, a finite element discretization with, for example, piecewise six-linear test and trial functions would lead to a discrete eigenvalue problem to be solved. If (after restricting the problem to a sufficiently large finite domain) we assume a spatial resolution by N grid points in each direction, then the size of the corresponding discrete eigenvalue problem will be proportional to N^6. We encounter the so-called curse of dimensionality. This renders the direct finite element discretization obsolete: For a reasonable value of N, the resulting problem cannot be stored and solved on any existing parallel computer because of its mere size.

However, there is a special discretization technique using so-called sparse grids which allows us to cope with the complexity of the problem, at least to some extent. This method has been originally developed for the solution of partial differential equations [5, 9, 24, 48] and is now used successfully also for integral equations [16, 23], interpolation and approximation [6, 22, 31, 43, 45], and integration problems [18]. In the information-based complexity community it is also known as "hyperbolic cross points" and the idea can even be traced back to [44]. For a d-dimensional problem, the sparse grid approach employs only $O(N(\log N)^{d-1})$ grid points in the discretization. It can be shown that an accuracy of $O(N^{-2}\log(N)^{d-1})$ can be achieved pointwise or with respect to the L_2- or L_∞-norm provided that the solution is sufficiently smooth. Thus, in comparison to conventional full grid methods, which need $O(N^d)$ points for an accuracy of $O(N^{-2})$, the sparse grid method can be employed also for higher-dimensional problems. The curse of dimensionality of full grid methods affects sparse grids much less. Note that there exist different variants of solvers working on sparse grids, each with its distinctive advantage and drawback. One variant is based on finite difference discretization [20, 40], another approach uses Galerkin finite element discretization [5, 9, 37], and the so-called combination technique [24] makes use of multivariate extrapolation [13].

In the following, we apply the sparse grid combination technique to the eigenproblem of hydrogen and helium in strong magnetic and electric fields. To this end we have to modify the original approach somewhat and have to adapt it to the solution of eigenproblems. It turns out that this new method for the numerical solution of the Schrödinger equation allows us to deal directly with the six-dimensional helium problem on available parallel computers. Furthermore, the results for hydrogen with and without strong magnetic and electric fields as well as helium with and without strong magnetic fields match the values from the recent literature quite well. Because the sparse grid combination technique employs a conventional grid size parameter, the results obtained on different refinement levels can be postprocessed in a classical extrapolation step which further improves on the results. This is usually not

possible for the other techniques. Furthermore, the combination method can be parallelized in a straightforward way; see [19, 21]. In contrast to the above-mentioned approaches, we do not make use of inherent symmetries of the system to reduce the number of dimensions of the problem nor do we employ specially developed basis sets. This allows our method to be used straightforwardly also in the case of helium in general magnetic *and* electric fields.

The remainder of this paper is organized as follows: In Section 2 we discuss our numerical approach for the numerical solution of the Schrödinger equation. We present the basic idea of the combination technique, show how it must be modified for the treatment of eigenvalue problems as they arise with hydrogen and helium under strong magnetic and electric fields, and give some remarks on the computational aspects of the implementation. In Section 3 we present the results of our numerical computations and compare them to those of other approaches. We first consider the hydrogen problem, impose a strong magnetic field on it, and treat also the case of magnetic and electric fields. Then we turn to the helium problem, consider it under a strong magnetic field, and show finally the result for a computation for helium with both magnetic and electric fields. Some concluding remarks close the paper.

2. NUMERICAL APPROACH

In this section we introduce the problem to be considered, present the main principles of the combination technique for sparse grids, discuss necessary modifications for it, and give some remarks on computational aspects of the implementation.

2.1. *The Eigenvalue Problem*

If we use the Born–Oppenheimer approximation and neglect the finite mass of the nucleus, the Hamiltonian for hydrogen in a strong magnetic field B_z along the z-axis and in a general electric field F reads

$$H = -\Delta - \frac{2}{|\boldsymbol{x}|} - 2i\beta \begin{pmatrix} y \\ -x \\ 0 \end{pmatrix} \cdot \nabla + 4\beta S + \beta^2(x^2 + y^2) + F \cdot \boldsymbol{x}, \tag{1}$$

where $\boldsymbol{x} = (x, y, z) \in \mathbb{R}^3$. Here, $-\Delta$ denotes the kinetic energy of the electron, the term $-2/|\boldsymbol{x}|$ gives its Coulomb potential energy in the field of the nucleus, $-2i\beta \cdot (y \ -x \ 0)^T \cdot \nabla$ denotes its Zeeman term, $4\beta S$ gives its spin energy, and $\beta^2(x^2 + y^2)$ gives its diamagnetic term. $F \cdot \boldsymbol{x}$ denotes the influence of the electric field F. The length is measured in units of the Bohr radius a_{Bohr} and energy is measured in Rydberg. The magnetic field strength is measured in $B_Z = 4.70107 \times 10^5$ T, β is the strength of the magnetic field which points in the z-direction, and the electric field strength is measured in $F_Z = 5.14 \times 10^{11}$ V/m. This is a Hamiltonian living in three dimensions. Note that for $F = \mathbf{0}$ and $\beta = 0$ we regain the classical Hamiltonian of a one particle system with no outer fields, i.e., a one-electron system with fixed nucleus.

For the helium atom in a strong magnetic field B_z along the z-axis and in a general electric field F, the Hamiltonian reads

$$H = \sum_{j=1}^{2} \left[-\Delta_j - \frac{2}{|\boldsymbol{x}_j|} - 2i\beta \begin{pmatrix} y_j \\ -x_j \\ 0 \end{pmatrix} \cdot \nabla + 4\beta S_j + \beta^2\left(x_j^2 + y_j^2\right) + F \cdot \boldsymbol{x}_j \right] + \frac{1}{|\boldsymbol{x}_1 - \boldsymbol{x}_2|},$$

where $\boldsymbol{x} = (\boldsymbol{x}_1, \boldsymbol{x}_2) \in \mathbb{R}^6$. This sum includes for both electrons their respective energies from Eq. (1) and the expression $\frac{1}{|\boldsymbol{x}_1 - \boldsymbol{x}_2|}$ corresponds to the electron–electron repulsion energy. We use charge-Z-scaled atomic units, i.e., Z^2 Rydberg as energy unit, and we measure length in a_{Bohr}/Z, where for the helium atom Z equals 2. The magnetic field strength is measured in $B_Z = Z^2 \times 4.70107 \times 10^5$ T; β is the strength of the magnetic field which points in the z-direction. The electric field strength is now measured in $F_Z = Z \times 5.14 \times 10^{11}$ V/m. Because relativistic effects on the energies of helium are smaller than the required level of accuracy for astrophysical applications we neglect spin–orbit coupling. This Hamiltonian now lives in six dimensions. Again note that for $\beta = 0$ and $F = 0$ we obtain the Hamiltonian of a two-particle system with no outer fields, i.e., a two-electron system with fixed nucleus.

In both cases we have to solve the associated stationary Schrödinger equation

$$Hu = Eu, \tag{2}$$

which is an eigenproblem in either three- or six-dimensional space. The function u denotes the wavefunction and E denotes the eigenvalue to be found. The boundary condition is

$$u(\boldsymbol{x}) \to 0 \quad \text{for} \quad |\boldsymbol{x}| \to \infty.$$

A conventional finite element discretization would now employ an equidistant grid $\Omega_{n,\dots,n}$ with mesh size $h_n = 2^{-n}$ for each coordinate direction. To make things feasible, we have to restrict the continuous problem on $\mathbb{R}^d$ to a problem on a finite domain. To this end we choose a sufficiently large box $\overline{\Omega} = [-a, a]^d$ and restrict the eigenproblem to it. This approximation is justified because the eigenfunctions u decay rapidly away from the origin and approach zero in the limit $|\boldsymbol{x}| \to \infty$. Therefore, as usual in many physics applications, we cut off the eigenfunctions on the boundary of Ω and set their values equal to zero there. It remains to find a proper value for a.

A finite element method with piecewise d-linear test and trial functions on grid $\Omega_{n,\dots,n}$ now would result in the discrete eigensystem

$$H_{n,\dots,n} u_{n,\dots,n} = \lambda_{n,\dots,n} M_{n,\dots,n} u_{n,\dots,n} \tag{3}$$

with mass matrix $M_{n,\dots,n}$, discrete Hamiltonian $H_{n,\dots,n}$, and discrete eigenvalues $\lambda_{n,\dots,n}$.

This problem might in principle be treated by an appropriate eigensolver like the Lanzcos method, the (Jacobi–) Davidson method, or some other suitable iterative method. For a sufficiently smooth continuous solution u, we then would obtain an error $e_{n,\dots,n} = u - u_{n,\dots,n}$ whose size in L_p-norms is of the order $O(h_n^2)$, $p = 1, 2, \infty$. The number of grid points would be of order $O(h_n^{-d})$ and, in the best case, if the most effective techniques like multigrid methods are used, the number of operations is of the same order. However, this direct application of a finite element discretization and an eigensolver for the arising discrete system is clearly not possible for a six-dimensional problem. The arising system cannot be stored and solved on even the largest parallel computers today.

2.2. *The Sparse Grid Combination Technique*

Therefore we proceed as follows: We discretize and solve the problem on a certain sequence of grids $\Omega_{i_1,\dots,i_d}$ with uniform mesh sizes $h_j = 2a \cdot 2^{-i_j}$ in the jth coordinate

direction. These grids may possess different mesh sizes for different coordinate directions. To this end, we consider all grids $\Omega_{i_1,\ldots,i_d}$ with

$$i_1 + \cdots + i_d = n + (d-1) - l, \quad l = 0, .., d-1, \quad i_j > 0.$$

The finite element discretization of (2) with piecewise d-linear test and trial functions then results in the discrete eigensystems

$$H_{i_1,\ldots,i_d} u_{i_1,\ldots,i_d} = \lambda_{i_1,\ldots,i_d} M_{i_1,\ldots,i_d} u_{i_1,\ldots,i_d} \tag{4}$$

with mass matrices $M_{i_1,\ldots,i_d}$, discrete Hamiltonians $H_{i_1,\ldots,i_d}$, and eigenvalues $\lambda_{i_1,\ldots,i_d}$. We then solve these problems by a feasible method. The discrete eigenfunctions $u_{i_1,\ldots,i_d}$ are contained in the space $S_{i_1,\ldots,i_d}$ of homogeneous piecewise d-linear functions on grid $\Omega_{i_1,\ldots,i_d}$.

Note that all these problems are substantially reduced in size in comparison to (3). Instead of one problem with size $\dim(S_{n,\ldots,n}) = O(h_n^{-d}) = O(2^{nd})$, we now have to deal with $O(d \cdot n^{d-1})$ problems of size $\dim(S_{i_1,\ldots,i_d}) = O(h_n^{-1}) = O(2^n)$. For any reasonable n, each problem fits nicely into the main memory of a modern workstation. Moreover, all these problems can be solved independently, which allows a straightforward parallelization on a coarse grain level; see [19]. Also, there is a simple but effective static load balancing strategy available [21].

Finally we linearly combine the results $u_{i_1,\ldots,i_d} \in S_{i_1,\ldots,i_d}$ from the different grids $\Omega_{i_1,\ldots,i_d}$ as follows:

$$u_n^c = \sum_{l=0}^{d-1} (-1)^l \binom{d-1}{l} \sum_{i_1+\cdots+i_d=n+(d-1)-l} u_{i_1,\ldots,i_d}. \tag{5}$$

The resulting function u_n^c lives in a so-called sparse grid space

$$S_n^c := \bigcup_{\substack{i_1+\cdots+i_d=n+(d-1)-l \\ l=0,\ldots,d-1}} S_{i_1,\ldots,i_d}.$$

This sparse grid space has $\dim(S_n^c) = O(h_n^{-1}(\log(h_n^{-1}))^{d-1})$. It is spanned by a piecewise d-linear hierarchical tensor product basis; see [9]. Note that the summation of the discrete functions from different spaces $S_{i_1,\ldots,i_d}$ in (5) involves d-linear interpolation which resembles just the transformation to a representation in this hierarchical product basis. For details see [20, 25].

For the two-dimensional case, we display the grids needed in the combination formula of level 4 in Fig. 1 and give the resulting sparse grid.

The corresponding eigenvalues are combined in the same manner:

$$\lambda_n^c := \sum_{l=0}^{d-1} (-1)^l \binom{d-1}{l} \sum_{i_1+\cdots+i_d=n+(d-1)-l} \lambda_{i_1,\ldots,i_d}. \tag{6}$$

This is possible because of their representation with the Rayleigh quotient.

For second-order elliptic PDE model problems, it was proven that the combination solution u_n^c is almost as accurate as the full grid solution $u_{n,\ldots,n}$; i.e., the discretization error satisfies

$$\left\| e_{n,\ldots,n}^c \right\|_{L_p} := \left\| u - u_n^c \right\|_{L_p} = O\left(h_n^2 \log\left(h_n^{-1}\right)^{d-1}\right),$$

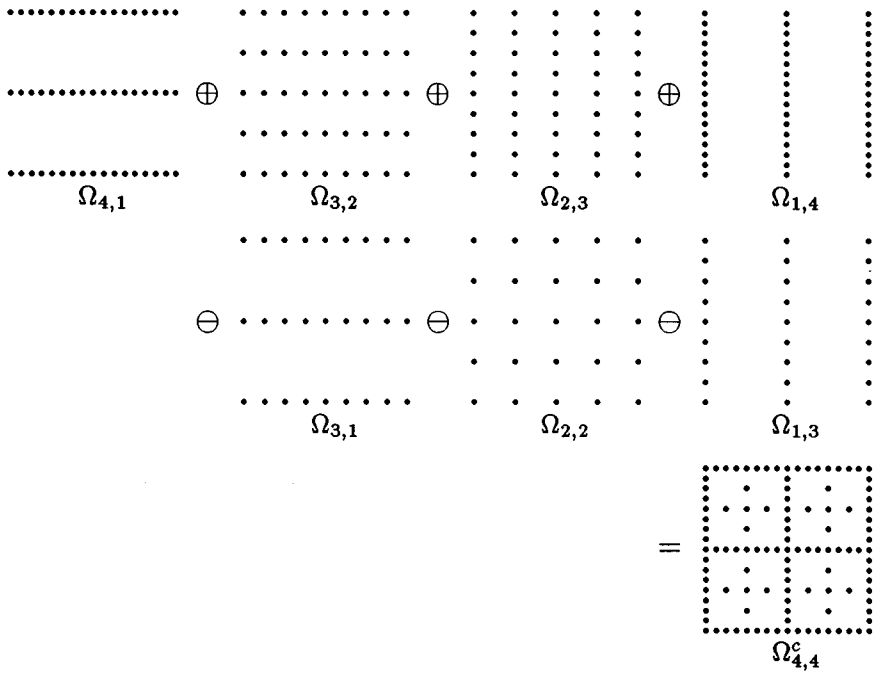

FIG. 1. Combination technique on level 4, $d = 2$, $l = 4$.

provided that a slightly stronger smoothness requirement on u than for the full grid approach holds. We need the seminorm

$$|u|_\infty := \left\| \frac{\partial^{2d} u}{\prod_{j=1}^{d} \partial x_j^2} \right\|_\infty \tag{7}$$

to be bounded. Furthermore, a series expansion of the error is necessary for the combination technique. Its existence was shown for PDE model problems in [12]. This approach should carry over to the eigenvalue problem without problems. Note that the combination technique can be interpreted as a certain multivariate extrapolation method which works on a sparse grid; for details see [13, 24, 38]. This also gives later the possibility of further improving on the results of the combination method by extrapolating the achieved results. The previously mentioned other approaches [7, 8] do not allow this.

The combination technique is only one of various methods to solve problems on sparse grids. There exist also finite difference [20, 40] and Galerkin finite element approaches [5, 9, 11] which work directly in the hierarchical product basis on the sparse grid. These methods allow adaptive local refinement of the sparse grid in a natural way. This cannot be achieved for the combination technique. However, the combination technique is conceptually much simpler and easier to implement. Moreover it allows the reuse of standard solvers for its different subproblems and is straightforwardly parallelizable.

2.3. *Identification of Eigenvalues*

Now the discrete eigenvalues and eigenfunctions have to be computed for every grid arising in the combination technique. For reasons of efficiency and complexity we do not

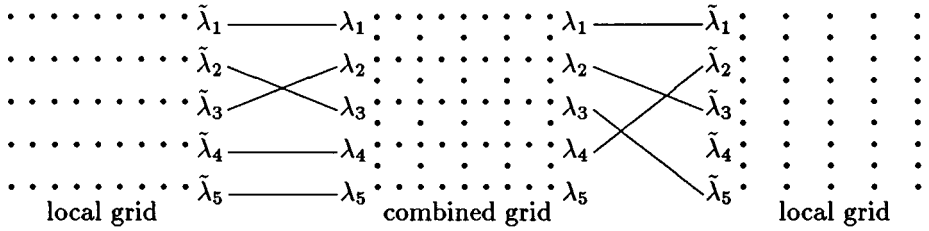

FIG. 2. The ordering of the eigenvalues for the combined grid does not need to correspond to the ordering on the grids used in the combination technique ($\lambda_i \leq \lambda_{i+1}$).

aim at the whole spectrum but merely settle for a sufficient amount eigenvalues and their associated eigenfunctions at the lower end of the spectrum. We employ a preconditioned version of the SIRQIT-CG [35] algorithm where we use a Jacobi preconditioner on the search directions of each eigenvalue.

Note that the combination formula (6) for the eigenvalues is not as straightforward as it seems. We encounter the following identification problem: The eigensolver computes on each grid the eigenfunctions in the ordering of the size of the eigenvalues. However, it may happen that the ordering of the discrete eigenvalues is different on the various grids of the combination technique. It is a priori not obvious which eigenvalue on one grid corresponds to which eigenvalue on an other grid; see Fig. 2 for a two-dimensional example. Therefore a procedure has to be developed to identify the respective eigenvalue on the different grids of the combination technique, before its values can be entered in the combination formula (6) to obtain the sparse grid approximation to the kth smallest eigenvalue of the continuous problem.

To this end, we proceed as follows: We define two grids to be "neighboring" if either their indices differ only in one coordinate direction by ± 1 or their indices differ in two coordinate directions, one by -1 and the other by $+1$. In other words we have either

$$\Omega_{i_1,\ldots,i_{k-1},i_k \pm 1,i_{k+1},\ldots,i_d}$$

for some $k \in \{1, \ldots, d\}$ or

$$\Omega_{i_1,\ldots,i_{p-1},i_p+1,i_{p+1},\ldots,i_{q-1},i_q-1,i_{q+1},,\ldots,i_d} \tag{8}$$

for some $p, q \in \{1, \ldots, d\}$, $p \neq q$, as the neighboring grids of $\Omega_{i_1,\ldots,i_d}$.

Furthermore we define an ordering of all the grids $\Omega_{i_1,\ldots,i_d}$ and their associated indices $(i_1, \ldots, i_d)$ arising in the combination technique by the following enumeration procedure:

$$\begin{aligned}
&l = 0 \text{ to } d-1\\
&\quad i_1 = 1 \text{ to } n-l\\
&\quad\quad i_2 = 1 \text{ to } n-l-(i_1-1)\\
&\quad\quad\quad i_3 = 1 \text{ to } n-l-(i_1-1)-(i_2-1)\\
&\quad\quad\quad\quad \ldots\ldots\\
&\quad\quad\quad\quad i_{d-1} = 1 \text{ to } n-l-(i_1-1)-\cdots-(i_{d-2}-1)\\
&\quad\quad\quad\quad\quad i_d = n-l-(i_1-1)-(i_2-1)-\cdots-(i_{d-2}-1)-(i_{d-1}-1).
\end{aligned}$$

Now, we traverse the set of grids according to this ordering. For each grid we pick that *neighboring* grid which was encountered most recently in the traversal. This gives us a unique sequence of pairs of neighboring grids.

We match the eigenfunctions (and thus their corresponding eigenvalues) of each pair of grids as follows: We interpolate the eigenfunctions (or alternatively their Fourier transforms) from the two respective grids to the finer grid which contains both grids (i.e., $\Omega_{i_1,\ldots,i_{p-1},i_p+1,i_{p+1},\ldots,i_d}$ in (8)) and we search there for the pairs of functions with the smallest distance measured in the Euclidean norm. This identifies their associated eigenvalues. This process starts with the grid $\Omega_{1,1,\ldots,n}$ and the desired eigenvalue there and traverses through the sequence of pairs of grids. Altogether this gives us the discrete eigenvalues needed for (6).

It is not clear to us if our approach always works. For example, for higher eigenvalues the shape of the eigenfunctions belonging to the same continuous eigenvalue might vary quite a lot from grid to grid, especially on strong anisotropic grids. This would result in intertwined eigenvalues.

A certain problem is the case of multiple eigenvalues. The eigenfunctions in the associated eigenspace are not unique and an identification is not possible. However, by imposing small perturbations on the problem we can cope with this effect; i.e., the multiple eigenvalues become numerically distinct and the eigenfunctions become unique. Of course, one has to take care that the introduced error stays smaller than the discretization error. To this end we slightly change the size of Ω with respect to the different coordinate directions. In all our numerical experiments, the introduced error was below the accuracy of the approximation but allowed multiple eigenvalues to be distinguished properly. Note furthermore that we did not use all grids of the combination technique in the case of multiple eigenvalues, because grids with a mesh size of $h_j = 2a \cdot 1/2$ only in at least one coordinate direction do not allow enough freedom to resolve multiple eigenvalues properly. Thus, we have to omit these grids from the combination process. The modified formula for the combination technique is then

$$u_n^c = \sum_{l=0}^{d-1} (-1)^l \binom{d-1}{l} \sum_{\substack{i_1+\cdots+i_d=n+(d-1)-l \\ i_j \geq ml+1}} u_{i_1,\ldots,i_d} \quad \text{with} \quad u_{i_1,\ldots,i_d} \in S_{i_1,\ldots,i_d},$$

with ml (=minimal level) being a parameter for the minimal number of points in one dimension on the subgrids. With $ml > 0$ the combination technique now involves fewer grids and the resulting sparse grid therefore has fewer points. Note that a similar modification of the combination technique was already used in the treatment of turbulent fluid flow problems; see [29].

Another difficulty is the following: In the presence of a magnetic field, i.e., if $\beta \neq 0$, the eigenfunctions $u_{i_1,\ldots,i_d}$ and consequently u_n^c are complex-valued. We avoid a complex-valued implementation of our sparse grid combination technique and handle their real and their imaginary part separately. We use the fact that the matrices are Hermitian and consequently the eigenvalues are real numbers. Thus we still can use our SIRQIT-CG eigensolver with only minimal modifications for handling the complex eigenfunctions. To this end we use the fact that an eigenvalue problem

$$\hat{A}\hat{x} = \begin{bmatrix} A_{\text{re}} & -A_{\text{im}} \\ A_{\text{im}} & A_{\text{re}} \end{bmatrix} \begin{bmatrix} x_{\text{re}} \\ x_{\text{im}} \end{bmatrix} = \lambda \begin{bmatrix} Mx_{\text{re}} \\ Mx_{\text{im}} \end{bmatrix} \tag{9}$$

has with eigenvector $\begin{bmatrix} x_{\text{re}} \\ x_{\text{im}} \end{bmatrix}$ also $\begin{bmatrix} -x_{\text{im}} \\ x_{\text{re}} \end{bmatrix}$ as eigenvector for the double eigenvalue λ. The composed matrix $\hat{A}$ is real and selfadjoint and possesses the eigenvalues of the original A just

twice; see also [47, p. 174]. So we call our eigensolver basically for a matrix with twice the size (real plus imaginary part) and can proceed as before. The previously described identification process of discrete eigenvalues by means of matching their eigenfunctions has to be modified accordingly. We now take the squares of the complex eigensolutions and compare them on neighboring grids in the identification routine. The squares of the eigenfunctions are the relevant informations for a physical interpretation anyway. Note that the identification of the eigenfunctions becomes more difficult the larger the magnetic field becomes. Then the orderings of the eigenvalues on the various grids of the combination technique become more and more intertwined. For example, in the case of hydrogen with magnetic field stronger than $\beta = 0.1$, we identified the first five eigenvalues. To achieve this it was necessary to compute up to 14 eigenvalues on the different grids of the combination technique.

2.4. *Graded Grids*

If the smoothness requirement (7) on the solution is not fulfilled, then the order $O(h_n^2(\log h_n^{-1})^{d-1})$ of the error of the sparse grid approximation can in general not be observed. Actually the order deteriorates to $O(h_n^r(\log h_n^{-1})^{d-1})$, where r resembles the corresponding smoothness of u. Note that for a finite element discretization on a full grid $\Omega_{n,\ldots,n}$ an analogous deterioration can be observed if its smoothness requirement, namely $\|\partial^2 u/\partial x_1^2 + \cdots + \partial^2 u/\partial x_d u\|_{L_p} \leq c < \infty$, or its equivalent weak form is not fulfilled. Then we only obtain an $O(h_n^r)$ order for the corresponding error.

In any case, for nonsmooth solutions, an adaptive refinement strategy can be employed to remedy the situation. The classical finite element method allows adaptive grid refinement in its h-version [3]. This technique has been successfully applied to the solution of the one-, two-, and three-dimensional Schrödinger equation for hydrogen and related one-particle systems; see [1, 2, 14]. Instead of finite elements, wavelets might be used also [34]. For a multigrid solver see [26]. Note, however, that because of the curse of dimensionality there is no hope for these methods ever to be applied to a six-dimensional problem. Adaptivity helps to cope with the nonsmooth behavior of the solution but cannot circumvent the intrinsic $O(N^6)$ complexity for the smooth parts of the solution. Besides, it is extremely difficult to define, to refine, and to code the necessary higher-dimensional adaptive data structures at all.

The sparse grid Galerkin method as well as the sparse grid finite difference method can be generalized to incorporate adaptive refinement strategies [5, 9, 11, 20, 40, 48, 49]. So far, the adaptive sparse grid Galerkin method has been applied successfully to the solution of the two- and three-dimensional Schrödinger equation for hydrogen and related ionized one-particle systems; see [27, 28]. But because of the extreme difficulty of coding differential operators more involved than the Laplacian and the more complicated potentials needed in the helium case, no implementations for higher-dimensional problems exist yet.

The generalization of the combination technique to adaptive local refinement is very difficult or even impossible. An easy way to obtain at least some a priori adaptive effect for the combination technique is to use graded instead of uniform grids; see also [25]. A grading function

$$g(x) \mapsto y, \quad x, y \in [a; b]$$

describes a certain change in the positions of the grid points. To this end, each point of the

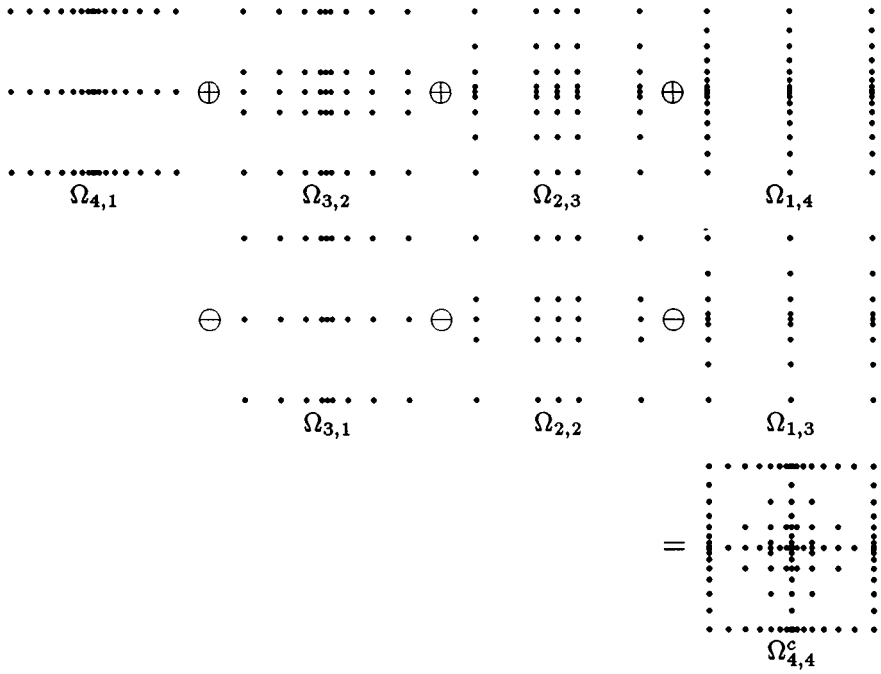

FIG. 3. Combination technique for a two-dimensional graded grid of level 4; the grading function is $g(x) = \text{sign}(x)x^2/a$ for every coordinate direction.

equidistant grid is mapped onto a point of the graded grid. Such a function can be applied in each coordinate direction independently, so that the resulting grid is still rectangular. Note that we roughly know a priori where more grid points are needed for the considered eigenproblems for hydrogen and helium. For the example of the Coulomb potential the area around the associated singularity is surely the region where a higher grid point density is appropriate.

Altogether, we allow a grading function to be prescribed for each coordinate direction. These functions map all the different grids arising in the combination formula accordingly and the combination technique then works on a graded sparse grid. An example for the grading induced by the Coulomb potential is given in Fig. 3. Of course, the formerly linear basis functions are transformed analogously and the linear interpolation between different grid spaces must be changed accordingly. For details see [25].

Surely, this approach is not optimal and merely a heuristic one. However, in practice it results in good improvements on the accuracy of the computed eigenfunctions and eigenvalues without much additional cost.

2.5. *Some Computational Aspects of the Implementation*

Let us now comment on the assembly of the stiffness matrices $H_{i_1,\ldots,i_d}$ on the various grids $\Omega_{i_1,\ldots,i_d}$ arising in the combination formula (5). To this end, each row of these matrices has about 3^d entries (except near boundaries). This is due to the d-linear test and trial functions we use in the finite element discretization process. While the component of the entries belonging to the kinetic energy, i.e., the Laplacian, can be given directly, the remaining parts of the Hamiltonian involve $\boldsymbol{x}$-dependent coefficient functions and need to

be evaluated numerically. Here, especially the computation of the six-dimensional expression resulting from the electron–electron repulsion energy $\frac{1}{|\boldsymbol{x}_1 - \boldsymbol{x}_2|}$ for helium is a tough numerical integration problem. We have

$$\int\int\int\int\int\int \frac{\phi_i(\boldsymbol{x})\phi_j(\boldsymbol{x})}{|\boldsymbol{x}_1 - \boldsymbol{x}_2|}\, d\boldsymbol{x}, \tag{10}$$

where $\phi_i(\boldsymbol{x})$, $\phi_j(\boldsymbol{x})$ denote six-linear test and trial functions. Not only does it involve an integration formula in six dimensions, but the integrand also exhibits a three-dimensional area singularity. A straightforward numerical integration with quadrature formulas is not possible in the parts of the integration domain where the pairs $\boldsymbol{x}_{1_i}$ and $\boldsymbol{x}_{2_i}$ overlap, $i = 1, 2, 3$.

Based on the work in [36] we developed recursion formulas for integrals of the type

$$\int\int\int\int\int\int \frac{x^k y^l z^m u^r v^s w^t}{|(x, y, z) - (u, v, w)|}\, dx\, dy\, dz\, du\, dv\, dw,$$

which make it possible to calculate the above integrals (10) accurately. For details see [17]. But the computations for the remaining parts of the integration domain are also quite costly because of the high dimensionality of the problem. Altogether, the integration of the entries of the stiffness matrices is a substantial factor in the total run time, and further savings are desirable. It must be further investigated if advanced quadrature techniques such as quasi-Monte Carlo or sparse grid integration [18] might help in this respect.

To reduce the computational work we can take advantage of the symmetry of the underlying potentials. This symmetry can be used in the integration of the stiffness matrix entries. Here integration results for some parts of the domain are just equal to those for certain other parts because of mirror symmetry. This substantially cuts the cost for the assembly of the system matrices which are needed in the combination technique.

3. NUMERICAL RESULTS

In this section we use the following notation: λ_n is a numerical eigenvalue at refinement level n, $e_n := \frac{|\lambda - \lambda_n|}{|\lambda|}$ is the relative eigenvalue error at level n in comparison to known exact solutions or results from other works taken as reference values, and $\delta\lambda_n := |\lambda_n - \lambda_{n-1}|$ is the difference between the corresponding numerical eigenvalues from level n and level $n - 1$.

3.1. *The Hydrogen Atom*

First we consider the Schrödinger equation for the hydrogen atom with no outer fields. Because of symmetry, the equation can be reduced to a one-dimensional problem for which an analytical solution is known. Nevertheless, the three-dimensional hydrogen equation is numerically demanding and therefore serves as a standard test problem for any numerical eigenvalue calculation of the Schrödinger equation. In the Born–Oppenheimer approximation we get the equation

$$-\Delta u(\boldsymbol{x}) - \frac{2}{|\boldsymbol{x}|} u(\boldsymbol{x}) = E u(\boldsymbol{x}). \tag{11}$$

Here length is measured in units of the Bohr radius a_{Bohr}, and energy is measured in Rydberg.

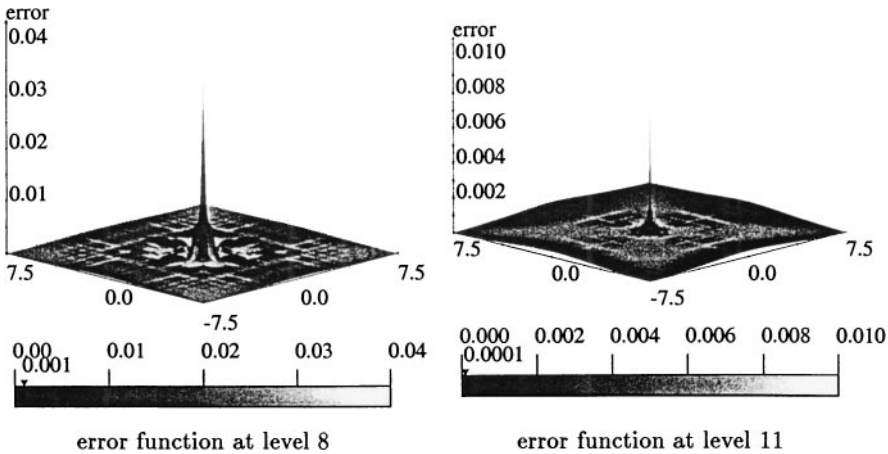

FIG. 4. Plot of the error function for the spatial probability distribution of the electron in the xy-plane for the ground state of the hydrogen atom at level 8 and 11.

Now we apply our sparse grid combination technique and compare its results to the known analytic values. To this end, we restrict the problem to the finite domain $[-a; a]^3$ and use homogeneous Dirichlet conditions on the boundary. To grade the sparse grid toward the origin we use the function $g(x) = \frac{\text{sign}(x)x^2}{a}$ for every coordinate direction; compare also Fig. 3. The Coulomb potential depends on the distance to the origin and, surely, the best would be a properly graded and rotationally symmetric grid around the origin. Such a configuration, however, cannot be achieved by the sparse grid combination technique. The grading of the grid is merely a heuristic which is not optimal but at least improves on the accuracy.

Figure 4 shows the xy-slice ($z = 0$) of the error function of the ground state for the resulting solutions at levels 8 and 11. Here, for display purposes, we used $a = 7.5$. For the computations reported in the following tables we used the value $a = 15$.

It can be clearly seen that the error is largest at the origin where the nucleus is situated. Here the solution develops a singularity. This singularity gets quite well isolated by the graded sparse grid, especially at the higher level. At the boundary of the computational domain we obtain an error by using homogeneous Dirichlet conditions there. This error is moderate but it becomes more important on finer levels.

Another source for error is the perturbation we impose in our identification process to distinguish the multiple eigenvalues when we calculate higher states ($2s$, $2p$). Here we change the domain to $[-a; a] \times [-a + \epsilon; a - \epsilon] \times [-a - \epsilon; a + \epsilon]$, with very small ϵ. Note that the induced error is significantly smaller than the accuracy of the approximation in all our experiments.

Table I shows the results for the calculation of the three smallest eigenvalues of the hydrogen problem. Note that the values for the three states $2p_0$, $2p_{-1}$, and $2p_{+1}$ are the same because of symmetry. We denote their common value by $2p$. We see that mostly an error quotient of 2 or slightly better is achieved. This suggests a convergence rate of $O(h_n^r \log(h_n^{-1})^2)$ with a value of r slightly larger than one, which is satisfactory for linear basis functions, and a severely nonsmooth eigensolution. We make the following remarks: First, the error introduced by the homogeneous Dirichlet boundary conditions on the boundary of $[-a, a]^3$ for $a = 15$ seems to influence the convergence rates starting with level 10.

TABLE I

The First Three Eigenvalues of the Hydrogen Atom: Graded Grid, *ml* = 1, *a* = 15

n	Points	Type	λ_n	e_n	$\frac{e_{n-1}}{e_n}$	$\delta\lambda_n$	$\frac{\delta\lambda_{n-1}}{\delta\lambda_n}$
4	27	1s	-0.7537644	$2.4624 \cdot 10^{-1}$	—	—	—
		2s	-0.1983182	$2.0673 \cdot 10^{-1}$	—	—	—
		2p	-0.1736482	$3.0541 \cdot 10^{-1}$	—	—	—
5	135	1s	-0.7711986	$2.2880 \cdot 10^{-1}$	1.0762	$1.7434 \cdot 10^{-2}$	—
		2s	-0.2025577	$1.8977 \cdot 10^{-1}$	1.0894	$4.2395 \cdot 10^{-3}$	—
		2p	-0.2095986	$1.6161 \cdot 10^{-1}$	1.8898	$3.5950 \cdot 10^{-2}$	—
6	495	1s	-0.8893831	$1.1106 \cdot 10^{-1}$	2.0684	$1.1818 \cdot 10^{-1}$	0.1475
		2s	-0.2244258	$1.0230 \cdot 10^{-1}$	1.8598	$2.2187 \cdot 10^{-2}$	0.1939
		2p	-0.2325699	$6.9720 \cdot 10^{-2}$	2.3179	$2.2971 \cdot 10^{-2}$	1.5650
7	1,567	1s	-0.9293292	$7.0670 \cdot 10^{-2}$	1.5652	$3.9946 \cdot 10^{-2}$	2.9586
		2s	-0.2357696	$5.6921 \cdot 10^{-2}$	1.7972	$1.1344 \cdot 10^{-2}$	1.9278
		2p	-0.2435165	$2.5934 \cdot 10^{-2}$	2.6884	$1.0947 \cdot 10^{-2}$	2.0985
8	4,543	1s	-0.9659534	$3.4047 \cdot 10^{-2}$	2.0757	$3.6624 \cdot 10^{-2}$	1.0907
		2s	-0.2428197	$2.8721 \cdot 10^{-2}$	1.9819	$7.0501 \cdot 10^{-3}$	1.6090
		2p	-0.2475368	$9.8530 \cdot 10^{-3}$	2.6321	$4.0202 \cdot 10^{-3}$	2.7229
9	12,415	1s	-0.9837864	$1.6214 \cdot 10^{-2}$	2.0998	$1.7833 \cdot 10^{-2}$	2.0537
		2s	-0.2465080	$1.3968 \cdot 10^{-2}$	2.0562	$3.6883 \cdot 10^{-3}$	1.9115
		2p	-0.2490494	$3.8023 \cdot 10^{-3}$	2.5913	$1.5126 \cdot 10^{-3}$	2.6577
10	32,511	1s	-0.9932130	$6.7870 \cdot 10^{-3}$	2.3889	$9.4266 \cdot 10^{-3}$	1.8918
		2s	-0.2484163	$6.3350 \cdot 10^{-3}$	2.2049	$1.9082 \cdot 10^{-3}$	1.9329
		2p	-0.2495858	$1.6570 \cdot 10^{-3}$	2.2948	$5.3635 \cdot 10^{-4}$	2.8203
11	82,431	1s	-0.9974147	$2.5853 \cdot 10^{-3}$	2.6253	$4.2017 \cdot 10^{-3}$	2.2435
		2s	-0.2492320	$3.0719 \cdot 10^{-3}$	2.0622	$8.1577 \cdot 10^{-4}$	2.3391
		2p	-0.2497760	$8.9596 \cdot 10^{-4}$	1.8496	$1.9028 \cdot 10^{-4}$	2.8187
12	203,775	1s	-0.9987955	$1.2045 \cdot 10^{-3}$	2.1464	$1.3808 \cdot 10^{-3}$	3.0430
		2s	-0.2495160	$1.9360 \cdot 10^{-3}$	1.5868	$2.8403 \cdot 10^{-4}$	2.8722
		2p	-0.2498424	$6.3040 \cdot 10^{-4}$	1.4218	$6.6420 \cdot 10^{-5}$	2.8648
Extrapolated		1s	-0.999759	$2.4062 \cdot 10^{-4}$	—	—	—
		2s	-0.249829	$6.8321 \cdot 10^{-4}$	—	—	—
		2p	-0.250007	$2.9601 \cdot 10^{-5}$	—	—	—
Exact		1s	-1.00	—	—	—	—
		2s	-0.25	—	—	—	—
		2p	-0.25	—	—	—	—

This is most obvious for the smooth $2p$-eigenfunction and the associated eigenvalue from column 6 of the table. In further experiments with larger values for a the onset of this effect was observed on higher levels. Then note the different convergence rates for the two types of second eigenvalues and their associated eigenfunctions. This is due to the different structure of the eigenfunctions. In Fig. 5 we show a cut through the two eigenfunctions for the second eigenvalue. Their different structure and smoothness properties can clearly be seen. This suggests that it would be appropriate to use for each eigenfunction its specially fitted grading function. Note that we use only one grading function for all eigenvalue problems. The grading function $\text{sign}(x)x^2/a$ is tailored to the Coulomb potential and the ground state. Therefore we lose out on the convergence rate of the much smoother $2p$-eigenfunction.

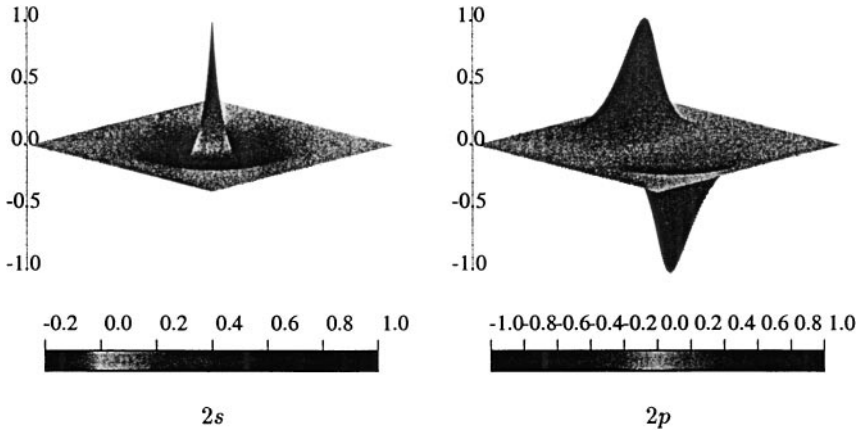

FIG. 5. Plot of the spatial probability distribution of the electron in the xy-plane for the second eigenfunctions, i.e., the states $2s$ and $2p_0$ of the hydrogen atom.

Here a compromise has been made between the adaptation of the grid to one eigenfunction and the overall convergence rate for the other eigenfunctions.

Furthermore, we see from Table I that the combination method is able to produce results on level 12 with a relative error of 10^{-3} to 10^{-4}, respectively. Here, with $ml = 1$, 109 different small eigenproblems have been solved with a size of only 14.415 interior points for the largest of them.

Because we employ a grid-based method and compute the results on different levels anyway, it makes sense to improve on the results by a further classical extrapolation step. To this end, we take the results on levels 9 to 12 into account, interpolate by means of a cubic polynomial, and evaluate this polynomial at the origin. The results are given in Table I (2nd row from below). Note that we gain more than one digit. This approach is legitimate because we employ a grid-based solution technique (h-version). It is not possible for the other approaches [7, 8].

3.2. *Hydrogen in Magnetic Fields*

We now consider hydrogen in a strong magnetic field. The equation to be solved is

$$\left(-\Delta - \frac{2}{|\boldsymbol{x}|} - 2i\beta \begin{pmatrix} y \\ -x \\ 0 \end{pmatrix} \cdot \nabla + 4\beta S + \beta^2(x^2 + y^2)\right) u = Eu, \quad \boldsymbol{x} \in [-a; a]^3. \tag{12}$$

We use the same finite domain size and grading function as in the previous subsection. The magnetic field strength is measured in $B_Z = 4.70107 \times 10^5$ T, β is the strength of the magnetic field which points in the z-direction, and S is the spin. Now, because of the magnetic field, this equation can be reduced by symmetry only to a two-dimensional problem for which an analytical solution is no longer known. Numerically very precise results for the eigenvalues of the hydrogen atom in strong magnetic fields were presented in [32, 39] for a wide range of field strengths. We consider in the following the original three-dimensional equation (12) to test our sparse grid combination method. The results for the first eigenvalue of hydrogen under the influence of a magnetic field of strength

TABLE II
First Eigenvalue of the Hydrogen Atom under the Influence of a Magnetic Field of Strength $\beta = 0.5$: Graded Grid, *ml* = 1

n	λ_n	e_n	$\frac{e_{n-1}}{e_n}$	$\delta\lambda_n$	$\frac{\delta\lambda_{n-1}}{\delta\lambda_n}$
4	-1.0451447	$3.7128 \cdot 10^{-1}$	—	—	—
5	-1.1005116	$3.3797 \cdot 10^{-1}$	1.0985	$5.5367 \cdot 10^{-2}$	—
6	-1.4457099	$1.3032 \cdot 10^{-1}$	2.5935	$3.4520 \cdot 10^{-1}$	0.1604
7	-1.5923373	$4.2110 \cdot 10^{-2}$	3.0947	$1.4663 \cdot 10^{-1}$	2.3543
8	-1.6293423	$1.9849 \cdot 10^{-2}$	2.1215	$3.7001 \cdot 10^{-2}$	3.9624
9	-1.6467572	$9.3728 \cdot 10^{-3}$	2.1177	$1.7415 \cdot 10^{-2}$	2.1249
10	-1.6555076	$4.1089 \cdot 10^{-3}$	2.2811	$8.7504 \cdot 10^{-3}$	1.9902
11	-1.6596830	$1.5971 \cdot 10^{-3}$	2.5727	$4.1754 \cdot 10^{-3}$	2.0957
12	-1.6609649	$8.2601 \cdot 10^{-4}$	1.9336	$1.2819 \cdot 10^{-3}$	3.2572
Extrapolated	-1.661035	$7.8384 \cdot 10^{-4}$	—	—	—
Corrected with Table I	-1.662170	$1.0142 \cdot 10^{-4}$	—	—	—

Reference value -1.662338 [39]

$\beta = 0.5$ are given in Table II. Table III shows the results for three eigenvalues for the case $\beta = 0.01$.

We obtain about the same convergence behavior as that for the case without a magnetic field. On level 12 we achieve a relative error in the range of 10^{-3} to 10^{-4}, and classical extrapolation improves on the result. Because the convergence rates for the computations with and without magnetic field are very similar, we think that it is justified to use the error of the case without magnetic field in a further correction step to the case with magnetic field. To this end, we take the error on level 12 of Table I and add it onto the result for the case with magnetic field. This approach results in a substantial improvement; see 2nd row from below in Tables II and III, which justifies our correction procedure a posteriori. The resulting eigenvalues are quite close to those presented in [39].

In Fig. 6 we give an example of the influence of a magnetic field on the form of two eigenfunctions ($2p_{-1}$ and $2p_0$). We show the isosurfaces of the spatial probability distribution $(u_n^c)^2/\|u_n^c\|^2$ of the electron for the values 0.2, 0.4, 0.6, and 0.8 under a magnetic field with strength $\beta = 0.0$, 0.01, and 0.3. Here, the direction of the magnetic field is parallel to the y-axis; we cut the isosurfaces open along the xz-plane.

3.3. *Hydrogen in Magnetic and Electric Fields*

We now consider the case of a magnetic and an electric field which both influence the electron of the hydrogen atom. To this end the potential term $\phi = F \cdot \boldsymbol{x}$ for the electric field F has to be added to (12). Note that our sparse grid combination approach can be directly applied without further modifications. This is not the case for most other methods for the calculation of energy values of the hydrogen atom in magnetic fields. Their adaptation to the case of a general additional electric field is not that easily, if at all, possible. The usually used reduction of the number of dimensions of the equation cannot be directly applied in the presence of both magnetic and electric fields. Here, the angle between these two fields is of relevance. With our approach, calculations for hydrogen in general magnetic fields and electric fields are straightforward. To be able to compare our results with results from the literature we stick to the simple case of parallel electric and magnetic fields in the following.

TABLE III

Three Eigenvalues of the Hydrogen Atom under the Influence of a Magnetic Field with Strength $\beta = 0.01$: Graded Grid, $ml = 1$

n	Type	λ_n	e_n	$\frac{e_{n-1}}{e_n}$	$\delta\lambda_n$	$\frac{\delta\lambda_{n-1}}{\delta\lambda_n}$
4	$1s$	-0.7734026	$2.4161 \cdot 10^{-1}$	—	—	—
	$2s$	-0.2132771	$2.0195 \cdot 10^{-1}$	—	—	—
	$2p_0$	-0.1897908	$2.9397 \cdot 10^{-1}$	—	—	—
5	$1s$	-0.7908242	$2.2453 \cdot 10^{-1}$	1.0761	$1.7422 \cdot 10^{-2}$	—
	$2s$	-0.2185629	$1.8217 \cdot 10^{-1}$	1.1086	$5.2857 \cdot 10^{-3}$	—
	$2p_0$	-0.2282972	$1.5072 \cdot 10^{-1}$	1.9504	$3.8506 \cdot 10^{-2}$	—
6	$1s$	-0.9091316	$1.0852 \cdot 10^{-1}$	2.0690	$1.1831 \cdot 10^{-1}$	0.1473
	$2s$	-0.2409273	$9.8489 \cdot 10^{-2}$	1.8497	$2.2364 \cdot 10^{-2}$	0.2363
	$2p_0$	-0.2515068	$6.4380 \cdot 10^{-2}$	2.3411	$2.3210 \cdot 10^{-2}$	1.6501
7	$1s$	-0.9491121	$6.9315 \cdot 10^{-2}$	1.5656	$3.9980 \cdot 10^{-2}$	2.9591
	$2s$	-0.2528442	$5.3898 \cdot 10^{-2}$	1.8273	$1.1917 \cdot 10^{-2}$	1.8767
	$2p_0$	-0.2624168	$2.3794 \cdot 10^{-2}$	2.7057	$1.0910 \cdot 10^{-2}$	2.1274
8	$1s$	-0.9857477	$3.3391 \cdot 10^{-2}$	2.0759	$3.6636 \cdot 10^{-2}$	1.0913
	$2s$	-0.2600765	$2.6836 \cdot 10^{-2}$	2.0084	$7.2323 \cdot 10^{-3}$	1.6477
	$2p_0$	-0.2663834	$9.0378 \cdot 10^{-3}$	2.6327	$3.9667 \cdot 10^{-3}$	2.7504
9	$1s$	-1.0035850	$1.5900 \cdot 10^{-2}$	2.1001	$1.7837 \cdot 10^{-2}$	2.0539
	$2s$	-0.2638049	$1.2885 \cdot 10^{-2}$	2.0827	$3.7284 \cdot 10^{-3}$	1.9398
	$2p_0$	-0.2678801	$3.3702 \cdot 10^{-3}$	2.6044	$1.4966 \cdot 10^{-3}$	2.6504
10	$1s$	-1.0130126	$6.6556 \cdot 10^{-3}$	2.3890	$9.4276 \cdot 10^{-3}$	1.8920
	$2s$	-0.2657138	$5.7423 \cdot 10^{-3}$	2.2439	$1.9089 \cdot 10^{-3}$	1.9532
	$2p_0$	-0.2684110	$1.4951 \cdot 10^{-3}$	2.3210	$5.3092 \cdot 10^{-4}$	2.8189
11	$1s$	-1.0172147	$2.5351 \cdot 10^{-3}$	2.6254	$4.2021 \cdot 10^{-3}$	2.2435
	$2s$	-0.2665285	$2.6937 \cdot 10^{-3}$	2.1318	$8.1473 \cdot 10^{-4}$	2.3430
	$2p_0$	-0.2685996	$7.9345 \cdot 10^{-4}$	1.8844	$1.8862 \cdot 10^{-4}$	2.8147
12	$1s$	-1.0185952	$1.1814 \cdot 10^{-3}$	2.1459	$1.3805 \cdot 10^{-3}$	3.0439
	$2s$	-0.2668115	$1.6332 \cdot 10^{-3}$	1.6485	$2.8304 \cdot 10^{-4}$	2.8784
	$2p_0$	-0.2686653	$5.4945 \cdot 10^{-4}$	1.4448	$6.5712 \cdot 10^{-5}$	2.8701
Extrapolated	$1s$	-1.019558	$2.3730 \cdot 10^{-4}$	—	—	—
	$2s$	-0.267125	$4.6025 \cdot 10^{-4}$	—	—	—
	$2p_0$	-0.268828	$5.5801 \cdot 10^{-5}$	—	—	—
Corrected	$1s$	-1.0197997	$2.9418 \cdot 10^{-7}$	—	—	—
with Table I	$2s$	-0.267296	$1.7961 \cdot 10^{-4}$	—	—	—
	$2p_0$	-0.268823	$3.7201 \cdot 10^{-5}$	—	—	—
Numerically	$1s$	-1.019800	—	—	—	—
precise [39]	$2s$	-0.267248	—	—	—	—
	$2p_0$	-0.268813	—	—	—	—

In Table IV we give the results obtained with the sparse grid combination technique for the second eigenvalue of the hydrogen atom in a magnetic field of strength $\beta = 0.01$ and a parallel electric field of strength $1.9455252 \times 10^{-4}\ F_Z$. We observe about the same convergence behavior as in the previous experiments. On level 12 we obtain a result with a relative error of 2.11×10^{-4} in comparison to a reference value taken from [15]. After extrapolation we obtain the value -0.269551 and after correction we get the value -0.269709, respectively. Because the rate $\frac{\delta\lambda_{n-1}}{\delta\lambda_n}$ from Table IV is almost the same as in Tables I and III

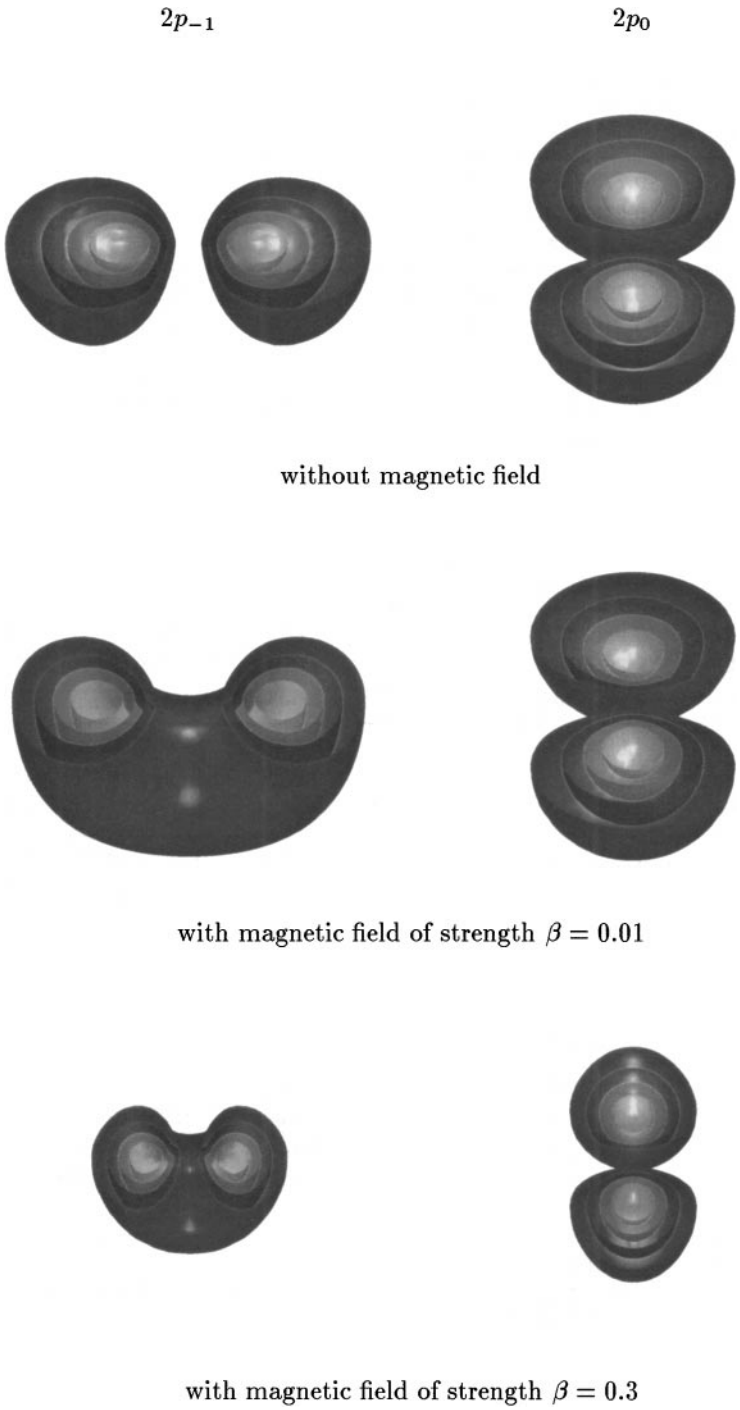

FIG. 6. Two second eigenfunctions of the hydrogen atom for different magnetic field strengths. Presented are the isosurfaces of the spatial probability distribution of the electron for the values 0.2, 0.4, 0.6, and 0.8 (from inside to outside). The direction of the magnetic field is parallel to the y-axis; the isosurfaces are cut open along the xz-plane.

TABLE IV

Second Eigenvalue of the Hydrogen Atom in a Magnetic Field of Strength $\beta = 0.01$ and a Parallel Electric Field of Strength $1.9455252 \times 10^{-4}\, F_Z$: Graded Grid, $ml = 1$

n	λ_n	e_n	$\frac{e_{n-1}}{e_n}$	$\delta\lambda_n$	$\frac{\delta\lambda_{n-1}}{\delta\lambda_n}$
4	-0.1908852	$2.9156 \cdot 10^{-1}$	—	—	—
5	-0.2292617	$1.4914 \cdot 10^{-1}$	1.9550	$3.8377 \cdot 10^{-2}$	—
6	-0.2522837	$6.3695 \cdot 10^{-2}$	2.3414	$2.3022 \cdot 10^{-2}$	1.6670
7	-0.2631517	$2.3360 \cdot 10^{-2}$	2.7266	$1.0868 \cdot 10^{-2}$	2.1183
8	-0.2671102	$8.6689 \cdot 10^{-3}$	2.6947	$3.9585 \cdot 10^{-3}$	2.7455
9	-0.2686045	$3.1231 \cdot 10^{-3}$	2.7758	$1.4943 \cdot 10^{-3}$	2.6490
10	-0.2691349	$1.1546 \cdot 10^{-3}$	2.7049	$5.3039 \cdot 10^{-4}$	2.8174
11	-0.2693234	$4.5501 \cdot 10^{-4}$	2.5375	$1.8848 \cdot 10^{-4}$	2.8140
12	-0.2693891	$2.1135 \cdot 10^{-4}$	2.1530	$6.5661 \cdot 10^{-5}$	2.8705
Extrapolated	-0.269551	$3.8960 \cdot 10^{-4}$	—	—	—
Corrected with Table I	-0.269709	$9.7450 \cdot 10^{-4}$	—	—	—

Reference value -0.269446 [15]

for the 2p case we infer an accuracy of 10^{-5} for the extrapolated eigenvalue. This indicates that the reference value is less precise than our result.

3.4. *The Helium Atom*

Now we consider the Schrödinger equation for the helium atom with no outer fields. In the Born–Oppenheimer approximation we have the six-dimensional equation

$$\left(\sum_{j=1}^{2}\left[-\Delta_j - \frac{2}{|\boldsymbol{x}_j|}\right] + \frac{1}{|\boldsymbol{x}_1 - \boldsymbol{x}_2|}\right) u = Eu, \quad \boldsymbol{x} = (\boldsymbol{x}_1, \boldsymbol{x}_2) \in [-a; a]^6,$$

to which we apply our sparse grid combination technique. In the following, we let $a = 15$ and choose the same grading function as previously; i.e., $g(x) = \mathrm{sign}(x)x^2/a$ for every coordinate direction. The parameter ml is set to 1. Note that the full combination technique, i.e., $ml = 0$, resulted in wrong results, and we had to use $ml = 1$ already for the ground state. It seems that the area singularity has too large an influence on grids where only one inner point is present in some dimensions. In contrast to other methods we make no use of symmetries to reduce the number of dimension but deal with the full six-dimensional equation instead.

The number of points of the grids $\Omega_{i_1,\ldots,i_d}$ dealt with in the combination technique is only of order $O(h^{-1})$ and the biggest of these grids on level 12 has only 50,421 inner points. Nevertheless, because we have a six-dimensional problem and use 6-linear test and trial functions, a row of the stiffness matrix has typically 729 nonzero entries (except near the boundary). On level 12 and with $ml = 1$ the biggest matrix has a size of 50,421, possesses 17,332,693 nonzero entries, and needs about 350 MB storage. The complete set of grids which make up this sparse grid has 2,534,913 inner points. With this level we reached the limit of the main memory of our computer. Because of the quite long run time needed for the setup of the matrix parts of the potential term (see the discussion in Section 2.5) at least these matrix data must be kept in memory and cannot be computed on

TABLE V
First Eigenvalue of Helium: Graded Grid, *ml* = 1

n	λ_n	e_n	$\frac{e_{n-1}}{e_n}$	$\delta\lambda_n$	$\frac{\delta\lambda_{n-1}}{\delta\lambda_n}$
7	-1.0811176	$2.5536 \cdot 10^{-1}$	—	—	—
8	-1.1366323	$2.1712 \cdot 10^{-1}$	1.1761	$5.5515 \cdot 10^{-2}$	—
9	-1.3102990	$9.7505 \cdot 10^{-2}$	2.2268	$1.7367 \cdot 10^{-1}$	0.3197
10	-1.3696518	$5.6624 \cdot 10^{-2}$	1.7220	$5.9353 \cdot 10^{-2}$	2.9251
11	-1.4192451	$2.2466 \cdot 10^{-2}$	2.5205	$4.9593 \cdot 10^{-2}$	1.1968
12	-1.4423054	$6.5824 \cdot 10^{-3}$	3.4130	$2.3060 \cdot 10^{-2}$	2.1506
Extrapolated	-1.443886	$5.4938 \cdot 10^{-3}$	—	—	—

Reference value -1.4518622 [4]

the fly. These memory limitations have prevented us so far from obtaining results on finer levels.

Table V gives the values for the first eigenvalue for helium computed with the combination technique. We see a reasonable convergence rate similar to that in the experiments for hydrogen. In comparison with a reference value from [4] we get on level 12 a relative accuracy of 6.58×10^{-3}. A classical extrapolation step involving the results from levels 9 to 12 gives even a slightly better value. However, surely, to improve on the result, computations on higher levels are necessary in the future. This requires a large parallel supercomputer.

3.5. *The Helium Atom in Strong Magnetic Fields*

First calculations for helium in strong magnetic fields were performed only in the past few years. The most accurate results so far were presented in [7], where a two-particle basis composed of one-particle states of a special Gaussian basis set was used. Similar accurate results were reached from a combination of the hyperspherical close coupling approach and a finite element method of quintic order [8]. Both methods involve a reduction in the dimension of the problem. In contrast, we treat in the following the full 6-dimensional equation for the helium atom in a strong magnetic field B_z along the z-axis,

$$\left(\sum_{j=1}^{2}\left[-\Delta_j - \frac{2}{|\boldsymbol{x}_j|} - 2i\beta\begin{pmatrix} y_j \\ -x_j \\ 0 \end{pmatrix}\cdot\nabla + 4\beta S_j + \beta^2\left(x_j^2 + y_j^2\right)\right] + \frac{1}{|\boldsymbol{x}_1 - \boldsymbol{x}_2|}\right)u = Eu, \tag{13}$$

where $\boldsymbol{x} = (\boldsymbol{x}_1, \boldsymbol{x}_2) \in [-a; a]^6$ with our sparse grid combination technique. Here, $a = 15$ was chosen. Furthermore, the grading function from the previous experiments was used again.

The results are displayed in Table VI. We obtain reasonable convergence results similar to the rates achieved before. On level 12 we achieve a relative accuracy of 6.89×10^{-3}. A classical extrapolation step gives only a slightly better value. Because the convergence rates for the computations with and without magnetic field are very similar, we think again that it is justified to take the error on level 12 of the case without magnetic field and use it to correct the new data. Similarly to the case of hydrogen, this approach resulted in a substantial improvement; see 2nd row from below in Table VI. With this defect correction, we obtain an eigenvalue which is quite near to the other results published in literature so far.

TABLE VI

First Eigenvalue of Helium in a Magnetic Field of Strength $\beta = 0.05$: Graded Grid, *ml* = 1

n	λ_n	e_n	$\frac{e_{n-1}}{e_n}$	$\delta\lambda_n$	$\frac{\delta\lambda_{n-1}}{\delta\lambda_n}$
7	-1.0521588	$2.6743 \cdot 10^{-1}$	—	-	—
8	-1.1114353	$2.2616 \cdot 10^{-1}$	1.1825	$5.9276 \cdot 10^{-2}$	—
9	-1.2937951	$9.9186 \cdot 10^{-2}$	2.2801	$1.8236 \cdot 10^{-1}$	0.3251
10	-1.3525565	$5.8273 \cdot 10^{-2}$	1.7021	$5.8761 \cdot 10^{-2}$	3.1034
11	-1.4032721	$2.2962 \cdot 10^{-2}$	2.5378	$5.0716 \cdot 10^{-2}$	1.1586
12	-1.4263453	$6.8970 \cdot 10^{-3}$	3.3293	$2.3073 \cdot 10^{-2}$	2.1980
Extrapolated	-1.427516	$6.0790 \cdot 10^{-3}$	—	—	—
Corrected with Table V	-1.435902	$2.4292 \cdot 10^{-4}$	—	—	—

Reference value -1.436251 [7] (-1.4363474 in [8])

In a series of experiments we computed the first eigenvalue of helium in a magnetic field for various values of β. For $\beta = 0.01, 0.025$, and 0.05 the results are given in Table VII.

For comparison, we also listed the numbers reported in other publications. We see that these results differ quite a bit. The other approaches surely have their own distinct sources of error (model approximations, discretization) whose influence on the final result is not completely understood. We believe that 3 to 4 reliable digits are state of the art. Our extrapolated and corrected results are therefore quite accurate and satisfactory.

3.6. *The Helium Atom in Strong Magnetic and Electric Fields*

Finally, we consider the problem of helium in strong magnetic and electric fields. To this end the term $\sum_{j=1}^{2} F \cdot \boldsymbol{x}_j$ must be added to the left-hand side of Eq. (13). Here we study the case of an electric field which is perpendicular to the magnetic field. The results obtained by the sparse grid combination technique are shown in Table VIII. We achieve a convergence behavior similar to that observed before.

In a further experiment we considered the case of helium under a magnetic field of strength $\beta = 0.05$ and a parallel electric field of strength 0.01. There we obtained the value -1.454730 for the first eigenvalue.

TABLE VII

Comparison of Energies for He at $\beta = 0.01$, 0.025 and 0.05 Obtained by Different Methods

	$\beta = 0.01$	$\beta = 0.025$	$\beta = 0.05$
This work (level 12)	-1.4416437	-1.4382257	-1.4263453
This work extrapolated	-1.443205	-1.439708	-1.427516
This work corrected with Table V	-1.451200	-1.4477832	-1.435902
Braun *et al.* [8]	-1.4512222	-1.4479	-1.4363474
Jones *et al.* [30]	-1.4302		-1.4155
Becken *et al.* [7]	-1.4510435		-1.436251
Thurner *et al.* [46]	-1.450975	-1.4476	-1.4357
Scrinzi *et al.* [42]		-1.4477	
Larsen *et al.* [33]		-1.4468	

TABLE VIII

First Eigenvalue of Helium in a Magnetic Field of Strength $\beta = 0.05$ and a Perpendicular Electric Field of Strength 0.01: Graded Grid, $ml = 1$

n	λ_n	e_n	$\frac{e_{n-1}}{e_n}$	$\delta\lambda_n$	$\frac{\delta\lambda_{n-1}}{\delta\lambda_n}$
7	−1.0748930	—	—	—	—
8	−1.1354310	—	—	$6.0538 \cdot 10^{-2}$	—
9	−1.3138772	—	—	$1.7845 \cdot 10^{-1}$	0.3393
10	−1.3719900	—	—	$5.8113 \cdot 10^{-2}$	3.0707
11	−1.4219477	—	—	$4.9958 \cdot 10^{-2}$	1.1632
12	−1.4448630	—	—	$2.2292 \cdot 10^{-2}$	2.1801
Extrapolated	−1.446180	—	—	—	—
Corrected with Table V	−1.454420	—	—	—	—

4. CONCLUSIONS

We presented the sparse grid combination technique for the calculation of eigenvalues of the Schrödinger equation for the hydrogen atom and the helium atom in magnetic and electric fields. In comparison to other methods we did not reduce the dimensions of the problem besides the standard Born–Oppenheimer approximation but directly treated the three- and the six-dimensional equation, respectively. For the hydrogen atom we obtained results which were almost equal to those in the literature which are considered to be numerically exact. Because of computer memory limitations we could not perform as precise calculations for helium as intended, but the results were still quite near to those published elsewhere. We admit that it is currently not possible to compute eigenvalues from the higher end of the spectrum. Also the grading of the grid, the extrapolation of the results, and the defect correction step is somewhat heuristic. But the important advantage of our approach is its universality. There is almost no difference in treating atoms with and without external fields. Without further modifications it was possible to calculate the eigenvalue of helium in the presence of magnetic *and* electric fields.

So far we have used only d-linear test and trial functions in the discretization step of the combination technique. A possibility for further improvement is the use of higher polynomials. Just d-quadratic test and trial functions should bring a substantial improvement in the accuracy; see also [10]. On the other hand we have to work further on the implementation if we ever want to treat higher-dimensional problems such as lithium, beryllium, and boron. The number of grid points involved in the combination technique is only of order $O(h_n^{-1}(\log(h_n^{-1}))^{d-1})$ and scales very moderately with d. But note that the order constant is exponentially dependent on d, at least as long as we use d-linear test and trial functions. Note finally that the treatment of higher-dimensional problems such as lithium, beryllium, and boron with the sparse grid combination technique is a future challenge for a large parallel supercomputer with many thousands of processors because the number of problems to be solved independently is of order $O(d \cdot (\log h_n^{-1})^{d-1})$.

REFERENCES

1. J. Ackermann, B. Erdmann, and R. Roitzsch, A self-adaptive multilevel finite element method for the stationary Schrödinger equation in three space dimensions, *J. Chem. Phys.* **101**, 7643 (1994).

2. J. Ackermann and R. Roitzsch, A two-dimensional multilevel adaptive finite element method for the time-dependent Schrödinger equation, *Chem. Phys. Lett.* **214**, 109 (1993).
3. I. Babuska and W. Rheinboldt, Error estimates for adptive finite element computations, *SIAM J. Numer. Anal.* **15**, 736 (1978).
4. J. D. Baker, D. E. Freund, R. N. Hill, and J. D. Morgan III, Radius of convergence and analytic behavior of the $1/z$ expansion, *Phys. Rev. A* **41**, 1247 (1990).
5. R. Balder, *Adaptive Verfahren für elliptische und parabolische Differentialgleichungen auf dünnen Gittern*. Dissertation (Institut für Informatik, Technische Universität München, 1994).
6. G. Baszenski, Nth order polynomial spline blending, in *Multivariate Approximation III* (edited by K. Zeller and W. Schemp, Birkäuser, Basel, 1985).
7. W. Becken, P. Schmelcher, and F. K. Diakonos, Helium in strong magnetic fields, *J. Phys. B* **32**, 1557 (1999).
8. M. Braun, W. Schweizer, and H. Elster, Hyperspherical close coupling calculations for helium in a strong magnetic field, *Phys. Rev. A* **57**, 3739 (1998).
9. H.-J. Bungartz, *Dünne Gitter und deren Anwendung bei der adaptiven Lösung der dreidimensionalen Poisson-Gleichung*, Dissertation (Institut für Informatik, Technische Universität München, 1992).
10. H.-J. Bungartz, *Finite Elements of Higher Order on Sparse Grids*, Habilitation (Institut für Informatik, Technische Universität München, 1998).
11. H.-J. Bungartz, T. Dornseifer, and C. Zenger, Tensor product approximation spaces for the efficient numerical solution of partial differential equations, in *Proc. Int. Workshop on Scientific Computations, Konya* (Nova Science Publishers, Inc., 1996).
12. H.-J. Bungartz, M. Griebel, D. Röschke, and C. Zenger, Pointwise convergence of the combination technique for the Laplace equation, *East-West J. Numer. Math.* **2**, 21 (1994).
13. H.-J. Bungartz, M. Griebel, and U. Rüde, Extrapolation, combination, and sparse grid techniques for elliptic boundary value problems, *Comput. Methods Appl. Mech. Eng.* **116**, 243 (1994).
14. E. Bylaska *et al.*, Scalable parallel numerical methods and software tools for material design, in *Proc. 7th SIAM Conf. on Parallel Processing for Scientific Computing, February 1995, San Francisco, CA, 1995*.
15. P. Faßbinder and W. Schweizer, The hydrogen atom in very strong magnetic and electric fields, *Phys. Rev. A* **53**, 2135 (1996).
16. K. Frank, S. Heinrich, and S. Pereverzev, Information complexity of multivariate Fredholm equations in Sobolev classes, *J. Complexity* **12**, 17 (1996).
17. J. Garcke, *Berechnung von Eigenwerten der stationären Schrödingergleichung mit der Kombinationstechnik* Diplomarbeit (Institut für Angewandte Mathematik, Universität Bonn, 1998).
18. T. Gerstner and M. Griebel, Numerical integration using sparse grids, *Numer. Algorithms* **18**, 209 (1998).
19. M. Griebel, The combination technique for the sparse grid solution of PDEs on multiprocessor machines, *Parallel Process. Lett.* **2**, 61 (1992).
20. M. Griebel, Adaptive sparse grid multilevel methods for elliptic PDEs based on finite differences, *Computing* **61**, 151 (1998).
21. M. Griebel, W. Huber, T. Störtkuhl, and C. Zenger, On the parallel solution of 3D PDEs on a network of workstations and on vector computers, in *Parallel Computer Architectures: Theory, Hardware, Software, Applications*, Lecture Notes in Computer Science, edited by A. Bode and M. Dal Cin (Springer-Verlag, Berlin/New York, 1993), Vol. 732, p. 276.
22. M. Griebel and S. Knapek, Optimized approximation spaces for operator equations, *Constr. Approx.* **16**, 525–540 (2000).
23. M. Griebel, O. Oswald, and T. Schiekofer, Sparse grids for boundary integral equations, *Numer. Math.* **83**, 279 (1999).
24. M. Griebel, M. Schneider, and C. Zenger, A combination technique for the solution of sparse grid problems, in *Iterative Methods in Linear Algebra*, edited by R. Beauwens and P. de Groen (Elsevier, Amsterdam/New York, 1992).
25. M. Griebel and V. Thurner, The efficient solution of fluid dynamics problems by the combination technique, *Int. J. Numer. Methods Heat Fluid Flow* **5**(3), 254 (1995).

26. F. F. Grindstein, H. Rabitz, and A. Askar, The multigrid method for accelerated solution of the discretized Schrödinger equation, *J. Comput. Phys.* **51**, 423 (1983).
27. S. Hilgenfeldt, *Numerische Lösung der stationären Schrödingergleichung mit Finite-Element-Methoden auf dünnen Gittern*, Diplomarbeit (Technische Universität München, 1994).
28. S. Hilgenfeldt, S. Balder, and C. Zenger, *Sparse grids: Applications to multi-dimensional Schrödinger problems*, Report SFB342 No. 342/05/95 (TU München, Institut für Informatik, 1995).
29. W. Huber, *Turbulenzsimulation mit der Kombinationsmethode auf Workstation-Netzen und Parallelrechnern*, Dissertation (Institut für Informatik, Technische Universität München, 1996).
30. M. D. Jones, G. Ortiz, and D. M. Ceperley, Hartree-Fock studies of atoms in strong magnetic fields, *Phys. Rev. A* **54**, 219 (1996).
31. S. Knapek, *Approximation und Kompression mit Tensorprodukt-Multiskalen-Approximationsräumen*, Dissertation (Institut für Angewandte Mathematik, Universität Bonn, 2000).
32. Yu. P. Kravchenko, M. A. Liberman, and B. Johansson, Exact solution for a hydrogen atom in a magnetic field of arbitrary strength, *Phys. Rev. A* **54**, 287 (1996).
33. D. M. Larsen, Variational studies of bound states of the H^- ion in a magnetic field, *Phys. Rev. B* **20**, 5217 (1979).
34. R. Lippert, T. Arias, and A. Edelman, Multiscale computations with interpolating wavelets, *J. Comput. Phys.* **140**, 278 (1998).
35. D. E. Longsine and S. F. McCormick, Simultaneous Rayleigh-quotient minimization method for $Ax = \lambda Bx$, *Linear Algebra Appl.* **34**, 195 (1980).
36. M. Maischak, *hp-Methoden für Randintegralgleichungen bei 3D-Problemen, Theorie und Implementierung*, Dissertation (Universität Hannover, 1995).
37. C. Pflaum, *Diskretisierung elliptischer Differentialgleichungen mit dünnen Gittern*, Dissertation (Institut für Mathematik, Technische Universität München, 1996).
38. C. Pflaum and A. Zhou, Error analysis of the combination technique, *Numer. Math.* **84**, 327 (1999).
39. H. Ruder, G. Wunner, H. Herold, and F. Geyer, *Atoms in Strong Magnetic Fields* (Springer-Verlag, Berlin/New York, 1994).
40. T. Schiekofer, *Die Methode der finiten Differenzen auf dünnen Gittern zur Lösung elliptischer und parabolischer PDEs*, Dissertation (Institut für Angewandte Mathematik, Universität Bonn, 1998).
41. P. Schmelcher and W. Schweizer, *Atoms and Molecules in Strong External Fields* (Plenum, New York, 1998).
42. A. Scrinzi, Helium in a cylindrically symmetric field, *J. Phys. B* **29**, 6055 (1996).
43. W. Sickel and F. Sprengel, Interpolation on sparse grids and tensor products of Nikol'skij-Besov spaces. *J. Comput. Anal. Appl.* **1**, 261 (1999).
44. S. Smolyak, Quadrature and interpolation formulas for tensor products of certain classes of functions, *Dokl. Akad. Nauk SSSR* **4**, 240 (1963).
45. V. Temlyakov, Approximation of functions with bounded mixed derivative, *Proc. Steklov Inst. Math.* **1** (1989).
46. G. Thurner, H. Herold, H. Ruder, G. Schlicht, and G. Wunner, Note on binding energies of helium-like systems in magnetic fields, *Phys. Lett.* **89A**, 133 (1982).
47. J. H. Wilkinson, *The Algebraic Eigenvalue Problem* (Oxford Univ. Press, London, 1965).
48. C. Zenger, Sparse grids, in *Parallel Algorithms for Partial Differential Equations, Proceedings of the Sixth GAMM-Seminar, Kiel, 1990*, edited by W. Hackbusch (Vieweg-Verlag, Wiesbaden, 1991).
49. G. Zumbusch, A sparse grid PDE solver, in *Advances in Software Tools for Scientific Computing*, Lecture Notes in Computational Science and Engineering, edited by H. P. Langtangen, A. M. Bruaset, and E. Quak (Springer-Verlag, Berlin/New York, 2000), Vol. 10, p. 133.